A polyalanine tract expansion in Arx forms intranuclear inclusions and results in increased cell death

Ilya M. Nasrallah,[1] Jeremy C. Minarcik,[2] and Jeffrey A. Golden[1,2]

[1]Neuroscience Program, University of Pennsylvania School of Medicine, [2]Department of Pathology, Children's Hospital of Philadelphia and the University of Pennsylvania School of Medicine, Philadephia, PA 19104

A growing number of human disorders have been associated with expansions of a tract of a single amino acid. Recently, polyalanine (polyA) tract expansions in the Aristaless-related homeobox (ARX) protein have been identified in a subset of patients with infantile spasms and mental retardation. How alanine expansions in ARX, or any other transcription factor, cause disease have not been determined. We generated a series of polyA expansions in Arx and expressed these in cell culture and brain slices. Transfection of these constructs results in nuclear protein aggregation, filamentous nuclear inclusions, and an increase in cell death. These inclusions are ubiquitinated and recruit Hsp70. Coexpressing Hsp70 decreases the percentage of cells with nuclear inclusions. Finally, we show that expressing mutant Arx in mouse brains results in neuronal nuclear inclusion formation. Our data suggest expansions in one of the ARX polyA tracts results in nuclear protein aggregation and an increase in cell death; likely underlying the pathogenesis of the associated infantile spasms and mental retardation.

Introduction

An increasing number of human diseases have been linked to the pathological expansion of normal tracts of single amino acid repeats. The first identified were associated primarily with polyglutamine repeats (La Spada et al., 1991; HDCRG, 1993; Zoghbi and Orr, 2000). Although the precise mechanism of pathogenesis of the expanded polyQ tracts is still unknown, these diseases share a number of similar characteristics, including formation of ubiquitinated inclusions, neural dysfunction, and cell type–specific cell death (Cummings and Zoghbi, 2000).

More recently, nine disorders have been associated with the expansion of a polyalanine (polyA) tract. In contrast to the polyQ repeat disorders, polyA tract expansions are most common in transcription factors. The one exception is polyadenosine binding protein nuclear 1, in which polyA expansions cause insoluble protein complexes that form nuclear inclusions in oculopharygeal muscular dystrophy (Brais et al., 1998; Calado et al., 2000; Fan et al., 2001). The other eight known polyA expansion disorders are characterized by developmental malformations ranging from defects in formation of digits (Synpolydactyly type II; Muragaki et al., 1996) to the central nervous system (Holoprosencephaly; Brown et al., 2001). Similarities between the phenotypes of polyA expansion mutations and null alleles suggest that the polyA-expanded proteins are at least partial loss of function mutations (Brown and Brown, 2004). However, the mechanism by which a polyA expansion in a transcription factor results in cellular dysfunction remains to be defined.

Expansions of polyA tracts in the *Aristaless-related homeobox* (*ARX*) have recently been identified in children with various neurological disorders (Stromme et al., 2002; Kato et al., 2004). *ARX* is expressed principally within the brain (Bienvenu et al., 2002; Kitamura et al., 2002) and contains five exons with four polyA tracts, a homeodomain, and a conserved "aristaless" domain (Miura et al., 1997). Deletions and truncation mutations are associated with X-linked lissencephaly with ambiguous genitalia (Kitamura et al., 2002; Uyanik et al., 2003). Patients with X-linked lissencephaly with ambiguous genitalia have severe structural anomalies of brain development and suffer from severe epilepsy and mental retardation (Dobyns et al., 1999; Bonneau et al., 2002). Expansions of the first polyA tract are associated with infantile spasms syndrome and mental retardation (ISSX/MR; Stromme et al., 2002; Kato et al., 2004). A similar phenotype is observed with loss of the 3′ aristaless domain (Stromme et al., 2002). Expansions of the second polyA tract cause a more variable phenotype including

Correspondence to Jeffrey A. Golden: goldenj@mail.med.upenn.edu

Abbreviations used in this paper: *Arx*, *Aristaless-related homeobox*; Arx^E, Arx with expanded polyA repeat; ISSX/MR, infantile spasms syndrome and mental retardation; polyA, polyalanine.

The Journal of Cell Biology, Vol. 167, No. 3, November 8, 2004 411–416
http://www.jcb.org/cgi/doi/10.1083/jcb.200408091

X-linked mental retardation and dystonia (Bienvenu et al., 2002). Here, we show expansion of the first polyA-tract in Arx results in protein accumulation with the formation of nuclear inclusions, which may be part of the cellular pathogenesis of ISSX/MR in patients with expansions in the first polyA tract of ARX.

Results and discussion

Expression of polyA-expanded Arx protein in vitro

We generated tagged expression constructs that increased the length of the first polyA tract from the normal of 15 (Miura et al., 1997) to 23 (referred to as Arx with expanded polyA repeat [Arx^E]), corresponding to the expansion found in patients with ISSX/MR (Kato et al., 2003; Fig. 1 a). Expression of wild-type Arx in COS or 293T cells results in diffuse nuclear expression of the protein (Fig. 1, e–g, and not depicted). In contrast, expression of Arx^E results in intranuclear aggregates of mutant protein in 25–35% of transfected cells (Fig. 1, b–d, and not depicted) even with similar levels of proteins expression (Fig. 4 and not depicted). One or two aggregates were found per cell, usually adjacent to the nuclear envelope. Frequently, little Arx^E could be detected throughout the remainder of the nucleus (Fig. 1 b). These aggregates were often observed to exclude chromatin (Fig. 1 c). Ultrastructural examination confirmed the intranuclear location of the protein and demonstrated fibril formation characteristic of nuclear inclusions (Fig. 1, h–j). A similar frequency and appearance of nuclear inclusions was observed with different epitope tags located at either the COOH or NH_2 terminus (not depicted). Transfected cells not forming nuclear inclusions expressed Arx^E in a pattern qualitatively similar to cells transfected with wild-type Arx.

Expression of 5′GFP-tagged Arx constructs allowed us to visualize the formation of nuclear inclusions over time (Video 1, available at http://www.jcb.org/cgi/content/full/jcb.200408091/DC1). In these time-lapse series, one can initially see the steady accumulation of mutant Arx throughout the nucleus. Inclusions were found to form in cells diffusely expressing Arx^E by the progressive consolidation of protein, first at the edge of the nucleus and next by redistributing all of the mutant protein over 4–6 h (Video 1).

Expanded Arx protein increases cell death in vitro

In diseases caused by polyQ expansions and one other polyA expansion, the formation of nuclear inclusions is accompanied by an increase in cell death (Cummings and Zoghbi, 2000; Fan et al., 2001). To test whether expression of Arx^E causes an increase in cell death, we determined the rate of cell death in transfected COS cells ($n = 8$ transfections for each construct at each time point; $n > 70$ transfected cells per time point). Although no significant difference in the rate of cell death was observed after 24 h, by 48 h an average of 3.6% of cells transfected with wild-type Arx were TUNEL-positive, whereas 5.2% of cells transfected with Arx^E were TUNEL-positive ($P = 0.048$; Fig. 2).

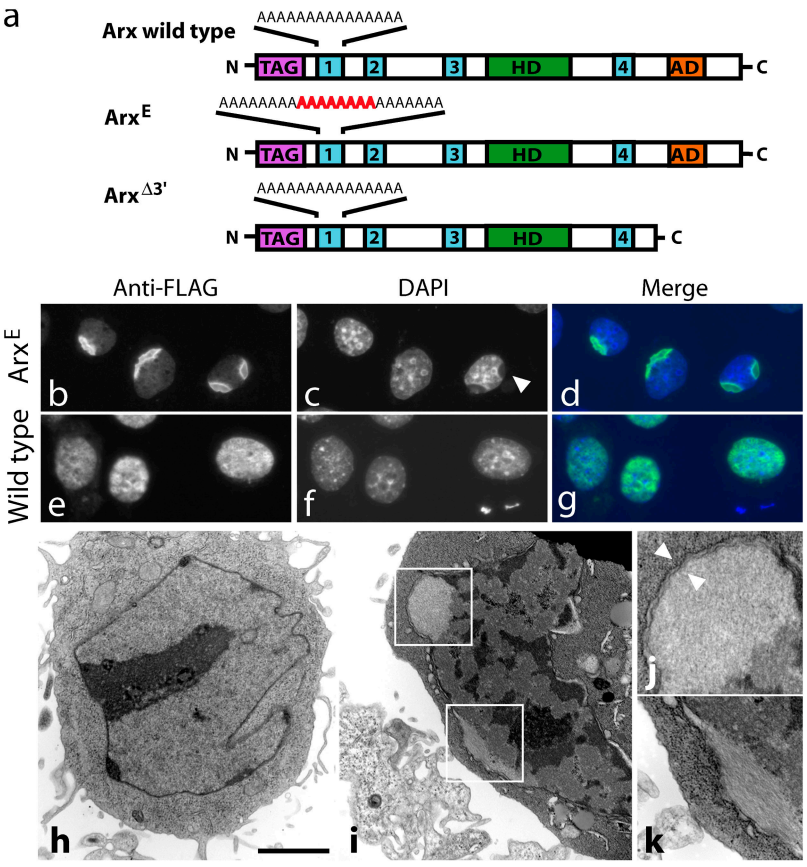

Figure 1. **Expression of Arx^E in COS cells leads to the formation of intranuclear inclusions.** (a) 5′ FLAG-tagged Arx expression constructs. The location of the homeodomain (HD), aristaless domain (AD) and four polyA repeats (blue) are shown. The first polyA repeat in the Arx^E construct has an additional eight residues. The $Arx^{\Delta 3'}$ construct contains the complete homeodomain, all four polyA repeats but lacks the aristaless domain. Arx^E frequently accumulates into inclusions (b) that deform chromatin (c, arrowhead; d, merge). Wild-type Arx is expressed diffusely within the nucleus (e) overlapping with chromatin (f and g). Compared with untransfected COS cells (h), ultrastructure analysis of Arx^E-expressing cells shows that inclusions (j and k, boxed enlarged) are within the nuclear membrane (j, arrowheads). (k) The inclusion shows a fibrillar internal structure. Bar: (b–g) 12 μm; (h and i) 2 μm; and (j and k) 700 nm.

Arx nuclear inclusions are ubiquitinated and suppressed by overexpression of Hsp70

Improper protein folding has been implicated in the cellular dysfunction associated with expanded polyQ diseases. Misfolded proteins are believed to aggregate, form inclusions, sequester other cellular proteins, and often cause cell death (Warrick et al., 1998; Evert et al., 1999; Stenoien et al., 1999). Normally, proteins known as molecular chaperones prevent protein misfolding while the ubiquitin–proteasome pathway removes old and misfolded proteins. Indeed, studies of polyQ expansions have found that nuclear inclusions are often ubiquitinated (Paulson et al., 1997b; Cummings and Zoghbi, 2000). We hypothesized that Arx^E within inclusions has a misfolded structure and is ubiquitinated.

Untransfected COS cells and those expressing wild-type Arx (Fig. 3 c) show faint ubiquitin staining primarily in the cytoplasm (Fig. 3 d and not depicted). The nuclei of these control cells are generally devoid of ubiquitin reactivity, but occasionally have one or two punctate areas of faint ubiquitin staining that are always located centrally (Fig. 3 d). In contrast, COS cells transfected with Arx^E constructs have strong immunoreactivity to ubiquitin at the periphery of the nucleus corresponding to the nuclear inclusions (Fig. 3, a and b). Interestingly, despite Arx^E expression throughout the nucleus in cells that do not form inclusions, we only detected ubiquitination when nuclear inclusions form.

In addition to being ubiquitinated, multiple studies have found that molecular chaperone proteins, such as Hsp70, colabel with misfolded mutant proteins in the nuclear inclusions found in HD and SCA (Cummings et al., 1998; Anderson et al., 1999; Wyttenbach et al., 2000). COS cells expressing Arx showed minimal colocalization of Arx with Hsp70 (Fig. 4, d–f), whereas cells transfected with Arx^E showed colocalization of Hsp70 with nuclear inclusions (Fig. 4, a–c). These data are also consistent with the hypothesis that protein misfolding may be responsible for the formation of Arx^E nuclear inclusions.

Previous studies have shown that overexpression of chaperones can prevent the formation of nuclear inclusions (Paulson et al., 1997a,b; Cummings et al., 1998; Stenoien et al., 1999; Wyttenbach et al., 2000; Auluck et al., 2002). To determine if molecular chaperones can prevent Arx^E-related nuclear inclusions, we cotransfected COS cells with Arx^E and Hsp70 ($n = 3$–6 transfections for each molar ratio of constructs and 70–140 transfected cells per time point per condition; Fig. 4 g). Approximately 30% of COS cells transfected with Arx^E alone or Arx^E with various doses of a control GFP construct show nuclear inclusion formation (Fig. 4 g). In contrast, overexpression of Hsp70 resulted in a dose-dependent reduction in the percent of cells with nuclear inclusions without decreasing the number of cells expressing Arx^E or the level of Arx^E protein expressed (Fig. 4 h and not depicted). Correlating the protein expression data (Fig. 4 h) with the immunofluorescence data on inclusion formation (Fig. 1), it is also clear that the expression of high levels of Arx without the polyA tract expansion cannot form inclusions.

Nuclear inclusion formation is specific to polyA-expanded ARX

Because many different mutations in *ARX* have been linked to ISSX/MR, we wondered whether all mutations predisposed ARX to form protein aggregates and nuclear inclusions, perhaps by causing improper protein folding. To test this hypothesis, we generated a 3′ deletion of *Arx* ($Arx^{\Delta 3'}$; Fig. 1 a) corresponding to a deletion that causes ISSX/MR in humans (Stromme et al., 2002). Expression of $Arx^{\Delta 3'}$ in COS cells resulted in no nuclear inclusions despite transfection efficiencies similar to those for Arx^E ($n = 3$ transfections; not depicted). These data suggest that polyA expansions and 3′ deletions of ARX likely cause ISSX/MR by distinct mechanisms.

Expanded Arx causes nuclear inclusion formation in cortical neurons

Finally, we sought to determine if Arx^E expression in neurons would also result in nuclear inclusion formation. During mammalian embryonic development, Arx is expressed in the fore-

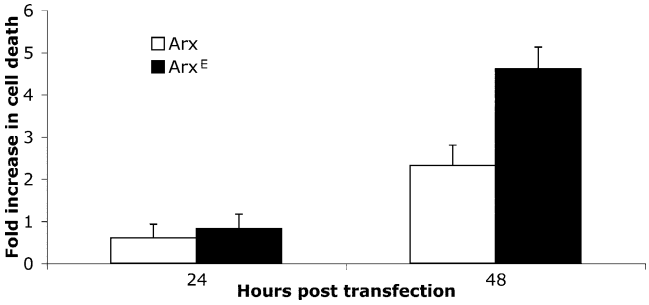

Figure 2. **PolyA expansion of Arx increases cell death in vitro.** COS cells were transfected with Arx or Arx^E and harvested 24 or 48 h later. At 48 h, the amount of cell death in transfected neurons between these two groups was significantly higher. * indicates $P < 0.05$.

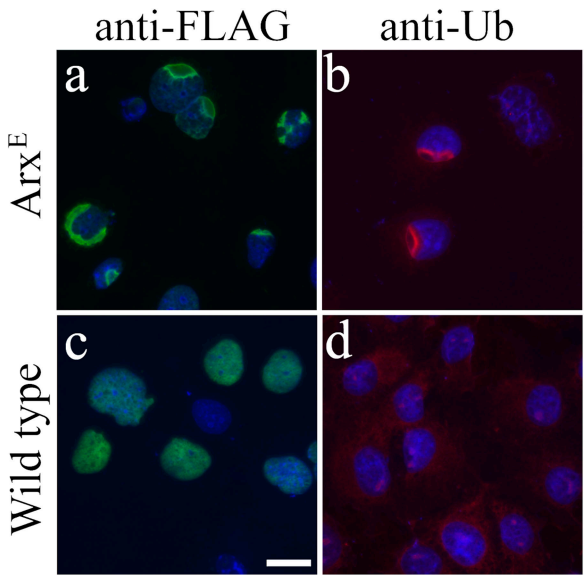

Figure 3. **Expanded Arx nuclear inclusions are ubiquitinated.** (a and b) COS cells expressing Arx^E aggregate Arx^E into nuclear inclusions (a). These nuclear inclusions stain positively for ubiquitin (b). (c and d) In contrast, cells expressing wild-type Arx do not form nuclear inclusions (c), nor do they show nuclear ubiquitin staining (d). Bar, 10 μm.

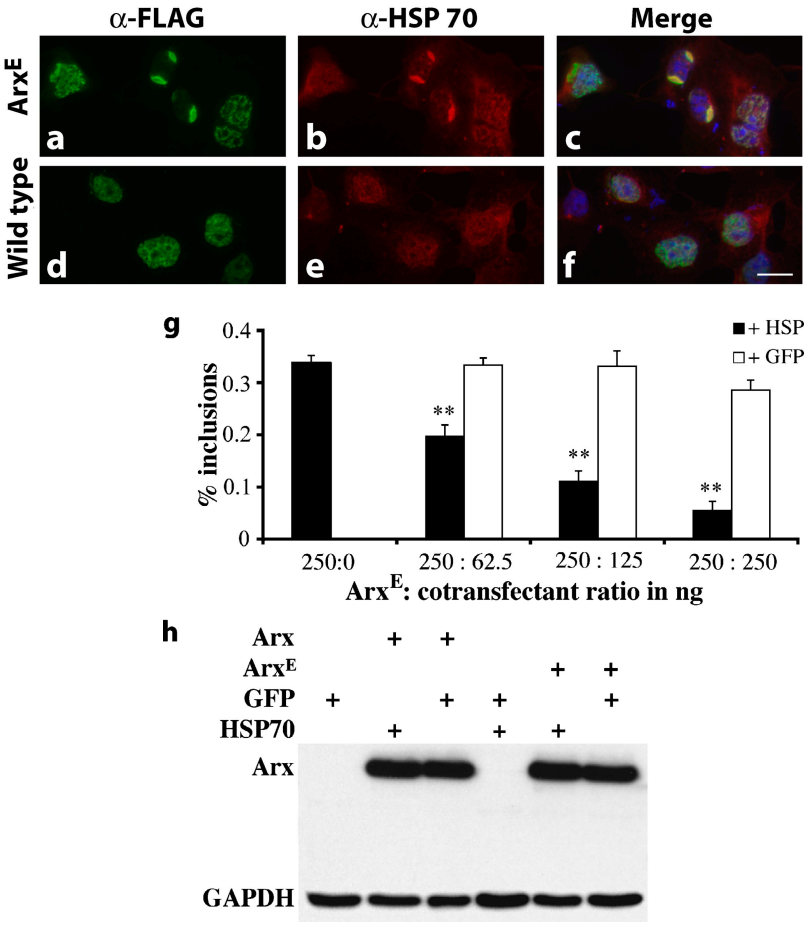

Figure 4. **Hsp70 colocalizes with Arx^E and reduces the number of cells with nuclear inclusions.** (a–c) Endogenous Hsp70 colocalizes with expanded Arx protein within nuclear inclusions in COS cells. Cells that have not formed nuclear inclusions, as well as cells transfected with wild-type Arx (d–f), have diffuse cytoplasmic and nuclear Hsp70 expression. Bar, 10 μm in a–f. (g) Cotransfection of Arx^E with an Hsp70 expression vector results in a dose-dependent decrease in transfected cells that have nuclear inclusions (solid bars) when compared with transfection of Arx^E alone (first bar on graph; ** indicates $P < 0.01$), or cotransfection with a GFP expression vector (open bars; same DNA concentrations as Hsp70). (h) Western blot analysis of COS cells transfected with a GFP expression vector or combinations of Arx or Arx^E and HSP70 or GFP. Expression levels of Arx and Arx^E are similar and do not change when HSP70 is coexpressed. Immunostaining for GAPDH shows equal protein loading between samples.

brain, the floor plate of the spinal cord, and the genital primordial (Miura et al., 1997; Kitamura et al., 2002; Ohira et al., 2002). Based on our in vitro data, we predicted that expression of Arx^E in forebrain neurons would result in nuclear protein aggregates and the formation of inclusions during development. By inducing neural dysfunction and cell death, these inclusions may contribute to the phenotype of ISSX and MR. Using whole brain electroporation, we expressed Arx^E in cortical neurons. When tagged wild-type *Arx* is expressed in cortical, subcortical, and hippocampal neurons, we observe diffuse nuclear expression of Arx protein (Fig. 5 a and not depicted). In contrast, expression of Arx^E in cortical neural populations results in the formation of nuclear inclusions in 8–22% of transfected neurons (Fig. 5, b–d).

Here, we have identified a novel mechanism by which polyA expansions of ARX may lead to human disease. PolyA tracts are commonly found in transcription factors; genomics analysis has identified polyA tracts in >300 human transcription factors (Karlin et al., 2002). By folding improperly, polyA-expanded ARX accumulates in intranuclear inclusions. Although mutations that eliminate or alter ARX activity and those that favor it being sequestered in inclusions may both directly decrease its ability to regulate transcription of as-yet undetermined targets, misfolded ARX may also coaggregate with other nuclear proteins and thereby have a "gain of function" effect. Such an effect is likely, given that one has been found for other diseases associated with nuclear inclusions (Ross et al., 1999). Furthermore, a dominant-negative activity has been identified in polyA-expanded HoxD13, which causes Synpolydactyly type II in part by altering the function but not expression of other Hox genes (Bruneau et al., 2001). Such an effect may be common to other polyA-expansion disorders and mediated by the formation of insoluble inclusions. Counter to the dominant negative hypothesis is the fact that loss of function mutations are more severe in patients and female carriers are rarely affected (Kato et al., 2004). Aberrant protein–protein interactions may be relevant to the pathogenesis of polyA expansion disorders even if inclusions are not identified in affected human cases, as it has been hypothesized that formation of macroscopic nuclear inclusions is not required for the pathogenesis of some polyQ disorders (Klement et al., 1998; Ross et al., 1999; Okazawa, 2003).

Materials and methods

Construction of expression constructs

Wild-type *Arx* cDNA was obtained from K. Kitamura (Institute of Life Sciences, Tokyo, Japan). Expansion of the first polyA tract was achieved by adding a short oligonucleotide duplex made by annealing two primers: 5′-ggccgctgctgctgctgccgc-3′ and 5′-ggccgcggcagcagcagcagcagc-3′ (IDT) into a unique NotI site within the region coding for the polyA tract. Wild-type and expanded *Arx* were individually subcloned in frame with 5′FLAG-, 5′Myc-, 5′GFP- and 3′V5-tagged expression constructs (pCMV-Tag2A (Stratagene), pCMV-Myc and pEGFP-C3 (CLONTECH Laborato-

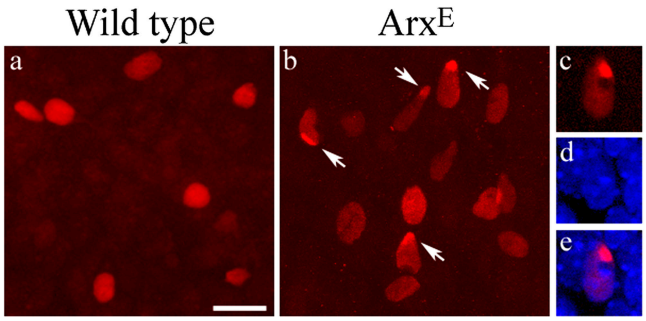

Figure 5. **Arx^E causes nuclear inclusion in cortical neurons.** Confocal microscopy of cortical neurons electroporated on E14.5 and immunostained for FLAG after 2 d in vitro. (a) Cortical neurons expressing FLAG-tagged wild-type Arx exhibit diffuse nuclear expression. (b) Cells expressing Arx^E often form nuclear inclusions (arrows). (c–e) Higher power of one nucleus shows an intensely staining inclusion along with faint diffuse nuclear staining for Arx^E. DAPI counterstaining (d) shows that the inclusion is located at the periphery of the nucleus (merge in e). In all frames, the ventricular surface is toward the top. Bar: (a and b) 25 μm; (c–e) 10 μm.

ries, Inc.), and pCDNA3.1-V5-His (Invitrogen), respectively; Fig. 1 a). To generate the 3′deleted constructs, *Arx* cDNA was digested with SalI to remove the 203 3′ bp of the 241-bp exon 5, including the aristaless domain (Fig. 1 a). Hsp70 cDNA was provided by N. Bonini (University of Pennsylvania, Philadelphia, PA) and cloned into pCDNA3.1.

Cell culture and video microscopy

COS and 293T cells were maintained in DME with 10% FBS and transfected using Fugene6 (Roche) and 500 ng of plasmid DNA. The cells were acid-alcohol fixed 2 d after transfection.

For time-lapse video microscopy, COS cells transfected with GFP-tagged constructs were placed on a Nikon TE-300 microscope equipped with a deltaT4 environmental chamber (Bioptechs) and a motorized stage (Prior) 6–18 h after transfection. A Nikon Plan Fluor ELWD 40×/0.6 lens was used for image acquisition. Using a CCD camera (Hamamatsu) controlled by Phase 3 Imaging Software (Media Cybernetics), fields were selected at random and fluorescent images were acquired every 15 min for 12–24 h. Phase 3 Imaging software compiled images into AVI files which were converted to MOV files in Quicktime Player 6.5.1.

Immunocytochemistry, TUNEL, and immunohistochemistry

Fixed cells were blocked with 10% normal goat serum (Sigma-Aldrich) in PBS and incubated with primary antibody. Primary antibodies included: mouse anti-FLAG M2 1:250 (Sigma-Aldrich), mouse anti-Hsp70 (1:300; StressGen Biotechnologies), mouse anti-myc 1:300 (9E10), and mouse anti-ubiquitin 1:500 (CHEMICON International Inc.). Secondary antibodies were species-appropriate FITC- or Texas red–conjugated raised in goat (1:150; Jackson ImmunoResearch Laboratories). Nuclei were counterstained with DAPI (Molecular Probes). The percent of transfected cells with inclusions was determined as the number of cells containing inclusions divided by the total number of FLAG-positive cells.

TUNEL staining was performed as described previously (Minarcik and Golden, 2003). In brief, fixed COS cells were blocked and incubated with TdT enzyme and UTP-biotin. Incorporation of UTP-biotin was labeled with streptavidin-Cy3 (Jackson ImmunoResearch Laboratories), and samples were immunostained as above. The percent of TUNEL-positivity in transfected cells was normalized to the percent of TUNEL-positivity in untransfected cells in order to control for the background rate of cell death for each transfection.

For immunohistochemistry of fixed embryonic brain slices, samples were blocked in PBS with 5% normal goat serum, 0.05% sodium azide, and 0.3% Triton X-100. They were incubated overnight at 4°C in primary antibody diluted in block, then incubated with secondary antibody in PBS. Nuclei were stained with DAPI.

Images were acquired on a DMR microscope (Leica) equipped with epifluorescence and an ORCA-ER CCD camera (Hamamatsu) connected to a Macintosh G4 running Openlab 3.1.5. The images were acquired using a Plan APO 40×/0.75 objective (Leica). Images were imported into Adobe Photoshop 7.0 and saved as TIF files. Some images were imported into Adobe Illustrator 10.0, labeled, and saved as EPS files.

Immunoblotting

Protein was extracted from cells using lysis buffer containing 25 mM Tris, pH 7.6, 1 mM $MgCl_2$, 1 mM EGTA, 1% Triton X-100, 1% PMSF, 50 μg/ml antipain, 2 μg/ml aprotinin, 1 μg/ml leupeptin, and 1 μg/ml peptastatin. The extract was homogenized using a 22-g needle and soluble protein was quantified with a BCA kit (Pierce Chemical Co.). These samples were then run on a 10% acrylamide SDS-PAGE gel with a 6% stacking gel. The separated proteins, including the stacking gel, were transferred to Immobilon membranes (Millipore). The membranes were incubated in block (5% NFDM, 0.1% Tween-20) followed by primary antibodies: anti-FLAG (1:1,000; Sigma-Aldrich) and anti-GAPDH (1:7500; CHEMICON International, Inc.) and HRP-conjugated secondary antibody (1:1,000; Amersham Biosciences). The blots were incubated in ECL buffer (Amersham Biosciences) and exposed to Kodak film. Quantification was performed with ImageJ.

Mouse brain electroporation

Whole brains from embryonic day 14.5–15 outbred CD1 mice were embedded in 4% low melting point agarose (Fisher Scientific). DNA was injected into one telencephalic ventricle and electroporated with three pulses of 40–60 mV using an ECM 830 electroporator and gold "Gene Paddle" electrodes (BTX). The brains were then cut at 250 μm on a vibrating microtome (model VT1000E; Leica). Brain slices were transferred to Millicell-CM filters (Millipore) and fed serum-containing medium for 2 h (1:1 DME/F12, Pen/Strep, 6.5 μM glucose, 10% FCS). Cultures were then grown for 2 d in serum-free medium (DME, Pen/Strep, 6.5 μM glucose, N2 supplement).

Online supplemental material

The dynamics of intranuclear inclusion formation were investigated by time-lapse video microscopy (Materials and methods). Mutant protein was first expressed throughout the nucleus at low levels followed by aggregation into dense inclusions. The development of inclusions was found to require many hours of mutant protein expression. Interestingly, the inclusions were dynamic, moving within the nucleus and able to form and disassemble. Video 1 is available at http://www.jcb.org/cgi/content/full/jcb.200408091/DC1.

We thank the other members of the Golden Lab for their support, discussions, and assistance.

This work was supported by HD26979 (to J.A. Golden), and institutional training grant GM07170 (to I.M. Nasrallah), and 5 F30 NS 6103-2 (to I.M. Nasrallah).

Submitted: 16 August 2004
Accepted: 29 September 2004

References

Anderson, S., M. Mione, K. Yun, and J.L. Rubenstein. 1999. Differential origins of neocortical projection and local circuit neurons: role of Dlx genes in neocortical interneuronogenesis. *Cereb. Cortex.* 9:646–654.

Auluck, P.K., H.Y. Chan, J.Q. Trojanowski, V.M. Lee, and N.M. Bonini. 2002. Chaperone suppression of alpha-synuclein toxicity in a Drosophila model for Parkinson's disease. *Science.* 295:865–868.

Bienvenu, T., K. Poirier, G. Friocourt, N. Bahi, D. Beaumont, F. Fauchereau, L. Ben Jeema, R. Zemni, M.C. Vinet, F. Francis, et al. 2002. ARX, a novel Prd-class-homeobox gene highly expressed in the telencephalon, is mutated in X-linked mental retardation. *Hum. Mol. Genet.* 11:981–991.

Bonneau, D., A. Toutain, A. Laquerriere, S. Marret, P. Saugier-Veber, M.A. Barthez, S. Radi, V. Biran-Mucignat, D. Rodriguez, and A. Gelot. 2002. X-linked lissencephaly with absent corpus callosum and ambiguous genitalia (XLAG): clinical, magnetic resonance imaging, and neuropathological findings. *Ann. Neurol.* 51:340–349.

Brais, B., J.P. Bouchard, Y.G. Xie, D.L. Rochefort, N. Chretien, F.M. Tome, R.G. Lafreniere, J.M. Rommens, E. Uyama, O. Nohira, et al. 1998. Short GCG expansions in the PABP2 gene cause oculopharyngeal muscular dystrophy. *Nat. Genet.* 18:164–167.

Brown, L.Y., and S.A. Brown. 2004. Alanine tracts: the expanding story of human illness and trinucleotide repeats. *Trends Genet.* 20:51–58.

Brown, L.Y., S. Odent, V. David, M. Blayau, C. Dubourg, C. Apacik, M.A. Delgado, B.D. Hall, J.F. Reynolds, A. Sommer, et al. 2001. Holoprosencephaly due to mutations in ZIC2: alanine tract expansion mutations may be caused by parental somatic recombination. *Hum. Mol. Genet.* 10:791–796.

Bruneau, S., K.R. Johnson, M. Yamamoto, A. Kuroiwa, and D. Duboule. 2001. The mouse Hoxd13(spdh) mutation, a polyalanine expansion similar to

human type II synpolydactyly (SPD), disrupts the function but not the expression of other Hoxd genes. *Dev. Biol.* 237:345–353.

Calado, A., F.M. Tome, B. Brais, G.A. Rouleau, U. Kuhn, E. Wahle, and M. Carmo-Fonseca. 2000. Nuclear inclusions in oculopharyngeal muscular dystrophy consist of poly(A) binding protein 2 aggregates which sequester poly(A) RNA. *Hum. Mol. Genet.* 9:2321–2328.

Cummings, C.J., and H.Y. Zoghbi. 2000. Trinucleotide repeats: mechanisms and pathophysiology. *Annu. Rev. Genomics Hum. Genet.* 1:281–328.

Cummings, C.J., M.A. Mancini, B. Antalffy, D.B. DeFranco, H.T. Orr, and H.Y. Zoghbi. 1998. Chaperone suppression of aggregation and altered subcellular proteasome localization imply protein misfolding in SCA1. *Nat. Genet.* 19:148–154.

Dobyns, W.B., E. Berry-Kravis, N.J. Havernick, K.R. Holden, and D. Viskochil. 1999. X-linked lissencephaly with absent corpus callosum and ambiguous genitalia. *Am. J. Med. Genet.* 86:331–337.

Evert, B.O., U. Wullner, J.B. Schulz, M. Weller, P. Groscurth, Y. Trottier, A. Brice, and T. Klockgether. 1999. High level expression of expanded full-length ataxin-3 in vitro causes cell death and formation of intranuclear inclusions in neuronal cells. *Hum. Mol. Genet.* 8:1169–1176.

Fan, X., P. Dion, J. Laganiere, B. Brais, and G.A. Rouleau. 2001. Oligomerization of polyalanine expanded PABPN1 facilitates nuclear protein aggregation that is associated with cell death. *Hum. Mol. Genet.* 10:2341–2351.

HDCRG. 1993. A novel gene containing a trinucleotide repeat that is expanded and unstable on Huntington's disease chromosomes. The Huntington's Disease Collaborative Research Group. *Cell.* 72:971–983.

Karlin, S., L. Brocchieri, A. Bergman, J. Mrazek, and A.J. Gentles. 2002. Amino acid runs in eukaryotic proteomes and disease associations. *Proc. Natl. Acad. Sci. USA.* 99:333–338.

Kato, M., S. Das, K. Petras, Y. Sawaishi, and W.B. Dobyns. 2003. Polyalanine expansion of ARX associated with cryptogenic West syndrome. *Neurology.* 61:267–276.

Kato, M., S. Das, K. Petras, K. Kitamura, K. Morohashi, D.N. Abuelo, M. Barr, D. Bonneau, A.F. Brady, N.J. Carpenter, et al. 2004. Mutations of ARX are associated with striking pleiotropy and consistent genotype-phenotype correlation. *Hum. Mutat.* 23:147–159.

Kitamura, K., M. Yanazawa, N. Sugiyama, H. Miura, A. Iizuka-Kogo, M. Kusaka, K. Omichi, R. Suzuki, Y. Kato-Fukui, K. Kamiirisa, et al. 2002. Mutation of ARX causes abnormal development of forebrain and testes in mice and X-linked lissencephaly with abnormal genitalia in humans. *Nat. Genet.* 32:359–369.

Klement, I.A., P.J. Skinner, M.D. Kaytor, H. Yi, S.M. Hersch, H.B. Clark, H.Y. Zoghbi, and H.T. Orr. 1998. Ataxin-1 nuclear localization and aggregation: role in polyglutamine-induced disease in SCA1 transgenic mice. *Cell.* 95:41–53.

La Spada, A.R., E.M. Wilson, D.B. Lubahn, A.E. Harding, and K.H. Fischbeck. 1991. Androgen receptor gene mutations in X-linked spinal and bulbar muscular atrophy. *Nature.* 352:77–79.

Minarcik, J.C., and J.A. Golden. 2003. AP-2 and HNK-1 define distinct populations of cranial neural crest cells. *Orthod. Craniofac. Res.* 6:210–219.

Miura, H., M. Yanazawa, K. Kato, and K. Kitamura. 1997. Expression of a novel aristaless related homeobox gene 'Arx' in the vertebrate telencephalon, diencephalon and floor plate. *Mech. Dev.* 65:99–109.

Muragaki, Y., S. Mundlos, J. Upton, and B.R. Olsen. 1996. Altered growth and branching patterns in synpolydactyly caused by mutations in HOXD13. *Science.* 272:548–551.

Ohira, R., Y. Zhang, W. Guo, K. Dipple, S. Shih, J. Doerr, B. Huang, L. Fu, A. Abu-Khalil, D. Geschwind, and E. McCabe. 2002. Human ARX gene: genomic characterization and expression. *Mol. Genet. Metab.* 77:179–188.

Okazawa, H. 2003. Polyglutamine diseases: a transcription disorder? *Cell. Mol. Life Sci.* 60:1427–1439.

Paulson, H.L., S.S. Das, P.B. Crino, M.K. Perez, S.C. Patel, D. Gotsdiner, K.H. Fischbeck, and R.N. Pittman. 1997a. Machado-Joseph disease gene product is a cytoplasmic protein widely expressed in brain. *Ann. Neurol.* 41:453–462.

Paulson, H.L., M.K. Perez, Y. Trottier, J.Q. Trojanowski, S.H. Subramony, S.S. Das, P. Vig, J.L. Mandel, K.H. Fischbeck, and R.N. Pittman. 1997b. Intranuclear inclusions of expanded polyglutamine protein in spinocerebellar ataxia type 3. *Neuron.* 19:333–344.

Ross, C.A., J.D. Wood, G. Schilling, M.F. Peters, F.C. Nucifora Jr., J.K. Cooper, A.H. Sharp, R.L. Margolis, and D.R. Borchelt. 1999. Polyglutamine pathogenesis. *Philos. Trans. R. Soc. Lond. B Biol. Sci.* 354:1005–1011.

Stenoien, D.L., C.J. Cummings, H.P. Adams, M.G. Mancini, K. Patel, G.N. DeMartino, M. Marcelli, N.L. Weigel, and M.A. Mancini. 1999. Polyglutamine-expanded androgen receptors form aggregates that sequester heat shock proteins, proteasome components and SRC-1, and are suppressed by the HDJ-2 chaperone. *Hum. Mol. Genet.* 8:731–741.

Stromme, P., M.E. Mangelsdorf, M.A. Shaw, K.M. Lower, S.M. Lewis, H. Bruyere, V. Lutcherath, A.K. Gedeon, R.H. Wallace, I.E. Scheffer, et al. 2002. Mutations in the human ortholog of Aristaless cause X-linked mental retardation and epilepsy. *Nat. Genet.* 30:441–445.

Uyanik, G., L. Aigner, P. Martin, C. Gross, D. Neumann, H. Marschner-Schafer, U. Hehr, and J. Winkler. 2003. ARX mutations in X-linked lissencephaly with abnormal genitalia. *Neurology.* 61:232–235.

Warrick, J.M., H.L. Paulson, G.L. Gray-Board, Q.T. Bui, K.H. Fischbeck, R.N. Pittman, and N.M. Bonini. 1998. Expanded polyglutamine protein forms nuclear inclusions and causes neural degeneration in Drosophila. *Cell.* 93:939–949.

Wyttenbach, A., J. Carmichael, J. Swartz, R.A. Furlong, Y. Narain, J. Rankin, and D.C. Rubinsztein. 2000. Effects of heat shock, heat shock protein 40 (HDJ-2), and proteasome inhibition on protein aggregation in cellular models of Huntington's disease. *Proc. Natl. Acad. Sci. USA.* 97:2898–2903.

Zoghbi, H.Y., and H.T. Orr. 2000. Glutamine repeats and neurodegeneration. *Annu. Rev. Neurosci.* 23:217–247.